

# Atrial Fibrosis Discernment via Hybrid 2D-3D Trans-Dilated ResUnet++ Leverages Echocardiographic Spatial-Temporal Encoding

P. Sudheer<sup>1</sup>, B. Kirubagari<sup>2</sup>, A. Annamalai giri<sup>3</sup>

<sup>1,2</sup>Department of Computer Science and Engineering, Annamalai University, Chidambaram, Tamil Nadu, India.

<sup>3</sup>Department of CSE, Marri Laxman Reddy Institute of Technology and Management, Telangana, India.

<sup>1</sup>Corresponding Author : [sudheerchanty7@gmail.com](mailto:sudheerchanty7@gmail.com)

Received: 10 September 2025

Revised: 12 October 2025

Accepted: 14 November 2025

Published: 28 November 2025

**Abstract** - Atrial fibrosis is a key pathological factor contributing to cardiac disorders such as Atrial Fibrillation (AF) and Congestive Heart Failure (CHF). AF, a prevalent arrhythmia in adults, significantly increases the risk of early mortality. Although various treatments-ranging from pharmacological interventions to surgical procedures-are available, the mechanisms driving AF and atrial fibrosis remain poorly understood. Moreover, distinguishing AF from normal sinus rhythm is complicated by signal noise and overlapping arrhythmic patterns. To address these diagnostic challenges, this study introduces a novel deep learning framework for early and accurate detection of atrial fibrosis. Initially, 2D echocardiographic images are collected from validated clinical sources. Feature extraction is performed using Convolutional Long Short-Term Memory (Conv-LSTM) networks, capturing fuzzy entropy, wavelet energy, hierarchical patterns, and deep semantic features. These are refined using the Hybrid Squirrel Crow Search Algorithm (HSCSA) to form Feature Set 1. Concurrently, sequential 2D frames are compiled into 3D volumes, forming Feature Set 2. Both feature sets are processed through a custom Hybrid Convolutional Transformer-Dilated Residual Unet++ (HC-TDRUnet++) model, which integrates 2D and 3D convolutional pathways for robust fibrosis detection. The proposed system demonstrates superior accuracy compared to existing models, offering a promising tool for managing AF and reducing the risk of stroke and heart failure.

**Keywords** - Segmentation of Atrial Fibrosis, Echocardiogram images, Optimal Feature Selection, Hybrid Squirrel Search, Crow Search Algorithms, Hybrid (2D, 3D) Convolution Transformer-Dilated Residual Unet++.

## 1. Introduction

The relation of AF with atrial fibrosis has been the subject of present research because it is the most frequently determined arrhythmia in adults. It considerably maximizes the premature death rate and stroke in humans [9]. Within the heart, one of the detrimental processes is cardiac fibrosis, which tends to imbalance the degradation and deposition of the Extracellular Matrix (ECM) and results in heavy fibroblast proliferation. In addition, there is the generation of ECM proteins in the space of the cardiac interstitial [1]. Much attention is received by ventricular fibrosis because it causes constant stiffening of the ventricular wall and results in CHF and ventricular dysfunction [2]. An Electrocardiogram (ECG) is the most effective and prevalent diagnostic method for identifying cardiac arrhythmia. AF is asymptomatic, and it is displayed in detail in the ECG signal, but it also remains challenging [3]. AF and atrial fibrosis are associated based on the pathway of drug targeting signaling, which also focuses on the therapeutic potential in analyzing the downstream and has the capability for more specific targets for fibrosis [4]. In

clinical practice, AF is the predominant arrhythmia, which is more common because of the growing population. With the growing risk of stroke, AF is widely associated with mortality and cardiovascular morbidity. For effective treatment, an accurate and early diagnosis is essential [5]. For the initial evaluation, Point-Of-Care Ultrasound (POCUS) machines or cart-based ultrasound devices are used in the echocardiography at the internal part. Here, the documented or non-documented palpitation patient requires AF or flutter for screening the arrhythmia based on the substrates [6]. In the present AF, the Intracardiac Echocardiography (ICE) is mostly incorporated into the catheter ablation. ICE is a significant tool based on its technological advancement to delineate the pericardial effusion and Left Atrial (LA) anatomy and rule out the Left Atrial Appendage (LAA) to perform flawless ablations [7]. The feasibility of the LA anatomy reconstruction is demonstrated either with individual ICE or combined with the CT to manage the ablation in Radiofrequency (RF) [8]. Other than these advantages, one of the major complexities generated by the ICE is the



maximization of time to fulfill the LA image, especially with a minimally experienced operator [9]. In the field of electrophysiology, Artificial Intelligence (AI) plays a major role, in which it automates the procedure for generating the LA anatomy with ICE to form more reproducible and accurate anatomical maps to guide the ablation [10]. The Two-Dimensional Echocardiogram (2DE) for the automatic Left Ventricular Ejection Fraction (LVEF) assessment is introduced. It can enhance reproducibility and save time when compared with the manual mechanism [11]. To solve the clinical needs, deep learning based algorithms are implemented for effective and automatic classification. For predicting heart disease, a fully automatic workflow is constructed to achieve high performance based on the ECG with degraded resolution [12]. Based on the deep learning mechanism, high-performance classification is achieved with high reproducibility [13]. The presence of structural variation and the rhythm minimized the accuracy and tended to complicate the clinical implications.

This includes the irregular cardiac cycle, dilation, motion abnormalities, and LV hypertrophy [14]. In addition, there is the requirement of large-scale variation and a considerable number of datasets to perform the robust deep learning mechanism, which is fully capable of performing different tasks in the clinical sector [15]. The existing models also faced complexities like the changes in the accuracy because of the suboptimal image quality [16]. Therefore, there is a need for a reliable and automatic detection model for effective atrial fibrosis identification.

The novel contributions of this study are represented below:

- To present a newly designed end-to-end hybrid deep learning architecture for the automatic segmentation process in identifying the AF based on the echocardiogram images. This segmentation model helps in identifying atrial fibrosis in the early stage and reduces structural heart complications like stroke and heart failure.
- To implement an HSCSA optimization approach for tuning the feature optimally. HSCSA is developed by the integration of two baseline algorithms, called SSA and CSA, with the adaptive concept. The process of feature tuning helps to attain the optimal feature selection, which tends to accurate segmentation.
- To design an HC-TDRUnet++ framework that performs the effective segmentation process by combining the transformer, residual, and Unet++ models. The optimal feature and the image series are processed through the (2D,3D) Convolution transformer, and the segmentation is carried out using the Runet++ structure. Compared with the standard approaches, the developed hybrid model attains robust segmentation.

The remainder of the paper is listed below. In Section II, the existing literature work for detecting AF is presented. Section III discusses the image collection and the description of the proposed model. Section IV describes the optimization algorithm and the feature selection process. Section V presented the segmentation process using the proposed deep learning model. Section VI defines the experimental setup and the corresponding comparative results. Section VII concludes the paper with future work.

## 2. Existing Works

### 2.1. Related Works

In 2024, Neal et al. [17] initiated the two-stage deep learning mechanism to predict AF by utilizing the CNN approach. Here, the video dataset was used, which has the sinus rhythm used for the detection process. The developed model could detect the concurrent paroxysmal sinus rhythm. From the analysis, the proposed mechanism performed better than the clinical measures by determining all the risk factors. Using the ECG signal along with the deep learning technique achieved better performance. From the result, the model could detect the occult or active AF by screening them, which helps in the early treatment.

In 2021, Bambang et al. [18] introduced the AF detection mechanism based on the CNN to achieve a powerful result. Without considering the different signals, the proposed approach utilizes a single learning model for sampling the frequency. A deep learning based computational cloud was implemented to process the data and function of the One-Dimensional CNN (IDCNN) to detect the AF. In the end, the obtained predicted value differentiated from the human practitioners' diagnosed result showed the specificity and the accuracy of the model.

In 2023, Biase et al. [19] determined the AF ablation to check the algorithm's feasibility based on the patient's CT. Here, the deep learning model was used to reconstruct the anatomical structure. The CT measurement measured the right and left pulmonary vein distance based on the ostial diameter. The LA anatomy's 3D reconstruction was generated by this algorithm based on the input frames from ultrasound. Without statistical significance, the carina-to-carina and mean ostial distance were differentiated. Based on this framework, all the ablation tends to succeed, and no sudden complications occur. In 2020, Tran et al. [20] proposed the deep learning-based Multi fusion network, which includes the trained deep neural network and the multiplicative fusion based on several sources of knowledge. The raw data were taken from the available resources, and the relevant features were extracted by the Multi Fusion Network to enhance the final process of the deep learning model. The accurate classification of AF was achieved by the experimental determination and outperformed based on the extracted feature. In the end, the result showed that the combination model outperformed other standard mechanisms.

In 2021, Liu et al. [21] designed a new deep learning model for automatic detection based on the 2DE images. The automatic generation of the LVEF measurement was evaluated based on the impact of phenotype and ultrasound machines on heart disease. The proposed network attained good agreements and high correlations for the LVEF measures. For the large-scale dataset, high performance was observed for suggesting the highly adaptive across multiple echocardiographic systems.

In 2020, Razeghi et al. [22] designed a multilabel CNN for the accurate detection of atrial structure, which consists of the mitral valve, blood pool, and pulmonary veins. The operator-dependent step was removed from the network output in the reproducible pipeline, and the automatic estimation of atrial fibrosis was performed. The obtained pipeline outcomes were differentiated against the manual fibrosis burdens based on the threshold value. The validation was conducted based on the LGE cardiac magnetic resonance data from the labeled scene.

In 2024, Lu et al. [23] proposed a diagnosis model based on the image assessment and ECG rhythm. From the standard dataset, the three cardiac cycle information were extracted, which includes the Doppler information and the rhythm strip, and introduced to the deep learning model. After training the deep learning model, the AI technique achieved high validation and accuracy for both sinus rhythm and AF. While comparing with the ECG assessment, the AF detection is performed based on the ECG rhythm strip. In 2021, Alugonda et al. [24] suggested a detection model based on deep learning to minimize false alarms at patient monitoring. By implementing the Pan-Tompkins Algorithm, the peak points from the ECG were identified. It gives the location information and amplitude. The accuracy of the reading was detected using the Deep Belief Network (DBN). Through AF detection, the rise in accuracy was ensured by patient protection for monitoring staff.

## 2.2. Research Gaps and Challenges

Fast and uneven heartbeats are the signs of AF. Patients may receive pharmaceutical treatment, atrioventricular node ablation, or catheter ablation to remove abnormal atrial tissue from clinicians. However, medication-based therapies have adverse consequences for patients. For healthy individuals, AF is typically less serious than other serious heart-related conditions. However, it is dangerous and results in fatalities if treatment is delayed. For this reason, it is crucial to accurately diagnose AF in the early stages. So, the researchers developed automatic atrial fibrosis detection models for precise detection, and some of the challenges in the existing models are presented below:

- The existing models utilized neural networks for the detection process of AF. However, this kind of network needs longer training time, and the cost requirement is also higher.
- Most of the conventional techniques use ECG for AF detection. However, the accuracy of those models is affected due to the presence of noise. So, cleaning the noise is crucial, and for the cleaning procedure, the ECGs should be segmented; it consumes a lot of time.
- Conventional methods are not effective in distinguishing between AF and sinus rhythm due to the absence of a feature extraction process.
- Even though some models used echocardiogram images, they are not capable of analyzing additional structural information needed for an accurate recognition of AF. So, using 2D or 3D echocardiography images is useful to obtain precise detection outcomes.
- Issues like determining the size of the left atrium and ventricles are complex, and they affect the consistency of the classification procedure, as the previous models do not utilize an effective optimization process.

Some of the features and challenges of the existing atrial fibrosis detection model using deep learning are listed in Table 1.

**Table 1. Features and challenges of the existing atrial fibrosis detection model using deep learning**

Author [citation]	Methodology	Features	Challenges
Neal et al. [17]	Deep Learning	<ul style="list-style-type: none"> <li>• This model effectively distinguishes between AF and sinus rhythm with high accuracy.</li> <li>• It can predict concurrent paroxysmal AF for earlier treatment and reduced stroke risk.</li> </ul>	<ul style="list-style-type: none"> <li>• Performs less well than ECG-based models.</li> <li>• It uses structural data, and it is not sufficient for obtaining accurate outcomes.</li> </ul>
Bambang et al. [18]	AFibNet	<ul style="list-style-type: none"> <li>• It performs well on different signal frequencies and lengths.</li> <li>• It has high reliability in recognizing AF, and it is suitable for real-time detection.</li> </ul>	<ul style="list-style-type: none"> <li>• It requires more computational resources due to cloud-based deployment.</li> <li>• Accuracy is slightly affected due to the imbalanced datasets.</li> </ul>

Biase et al. [19]	Deep Learning Algorithm	<ul style="list-style-type: none"> <li>It reduces the need for manual contouring.</li> </ul>	<ul style="list-style-type: none"> <li>It analyzes frames with 90–120 mm depth and does not support uncommon anatomical variations.</li> <li>This technique does not provide voltage map data, which is crucial for some procedures.</li> </ul>
Tran et al. [20]	Multi Fusion Net	<ul style="list-style-type: none"> <li>It integrates the raw data and extracts features for obtaining accurate AF classification results.</li> <li>It performs well even with noisy data and small training datasets.</li> </ul>	<ul style="list-style-type: none"> <li>Requires careful tuning of multiple sub-networks and fusion methods.</li> <li>It takes more time due to the depth and complexity of the model.</li> </ul>
Liu et al. [21]	U-Net	<ul style="list-style-type: none"> <li>The time needed for tracking the endocardial borders is low.</li> <li>It obtains high performance even with variations in image quality and different ultrasound systems.</li> </ul>	<ul style="list-style-type: none"> <li>Automatic measurement of LVEF is not possible.</li> </ul>
Razeghi et al. [22]	Multilabel Convolutional Neural Network	<ul style="list-style-type: none"> <li>It reduces the analysis time of AF.</li> </ul>	<ul style="list-style-type: none"> <li>It requires high-quality images to attain high accuracy.</li> </ul>
Lu et al. [23]	ResNet	<ul style="list-style-type: none"> <li>It has high consistency in detecting AF from echocardiography, which is helpful for earlier treatments.</li> </ul>	<ul style="list-style-type: none"> <li>The model's accuracy is low as it is not effective in input images with varying quality.</li> </ul>
Alugonda et al. [24]	DBN	<ul style="list-style-type: none"> <li>It minimizes the number of false alarms.</li> <li>It has the potential to handle complex data effectively.</li> </ul>	<ul style="list-style-type: none"> <li>Analyzing the features of AF with high accuracy is complex.</li> </ul>

### 3. Input Image Collection and Proposed Model Description for Atrial Fibrosis Disease Segmentation

#### 3.1. 2D Echocardiogram Images

For diagnosing diseases related to cardiovascular conditions like Atrial Fibrosis, echocardiography is an efficient imaging process that serves as the backbone of the detection mechanism. It is the readily available and widely used imaging technique to analyze the structure and function of the heart.

Therefore, this work utilizes echocardiography imaging from available data resources, which are explained below. The EchoNet-Dynamic database was taken from the link "[https://stanfordaimi.azurewebsites.net/datasets/834e1cd1-](https://stanfordaimi.azurewebsites.net/datasets/834e1cd1-92f7-4268-9daa-d359198b310a)

92f7-4268-9daa-d359198b310a Access Date: 2024-10-17. It is a huge video dataset of echocardiograms for the determination of computer vision.

The dataset contains the annotations of human experts and image series of echocardiograms to analyze the chamber size and the cardiac motion.

From the dataset, the 2D echocardiogram images are collected. From the dataset, the collected images are specified as  $Af_s^{ec}$ , where  $s = 1, 2, 3, \dots, S$ .

The term  $S$  is the total count of the collected image series. Figure 1 defines the sample 2D images collected from the presented dataset.

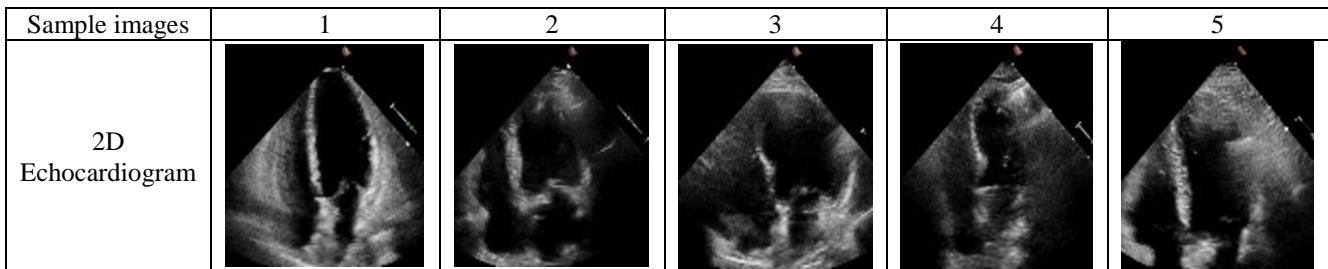


Fig. 1 Sample 2D echocardiogram images for Atrial Fibrosis segmentation

### 3.2. Description of Novel Segmentation Model

One of the most extensive cardiac arrhythmias is the AF, which affects adults all over the world. Because of the extended lifespan of the population, the prevalence has increased, and efforts have been made to detect undiagnosed AF cases. Some general pathophysiologic mechanisms coexist in cardioembolic stroke and AF. This AF can be identified based on non-invasive mechanisms like the MRI, Transthoracic Echocardiogram, and ECG through a highly dense electro-anatomical process. Various Pathological conditions utilize this disruption under different conditions

based on the physiological states. Various algorithms and detection models have been developed for diagnosing AF in the existing research. Multiple statistical measures are employed to evaluate the performance. Machine learning and deep learning algorithms are rapidly developing fields because of their simplified and robust structure. It can handle the complex tasks. But still, there is a huge challenge in the image segmentation process, which tends to poor grouping based on the image quality. Therefore, it is essential to develop an effective mechanism for the segmentation of AF. Figure 2 shows the designed framework for effective AF segmentation.

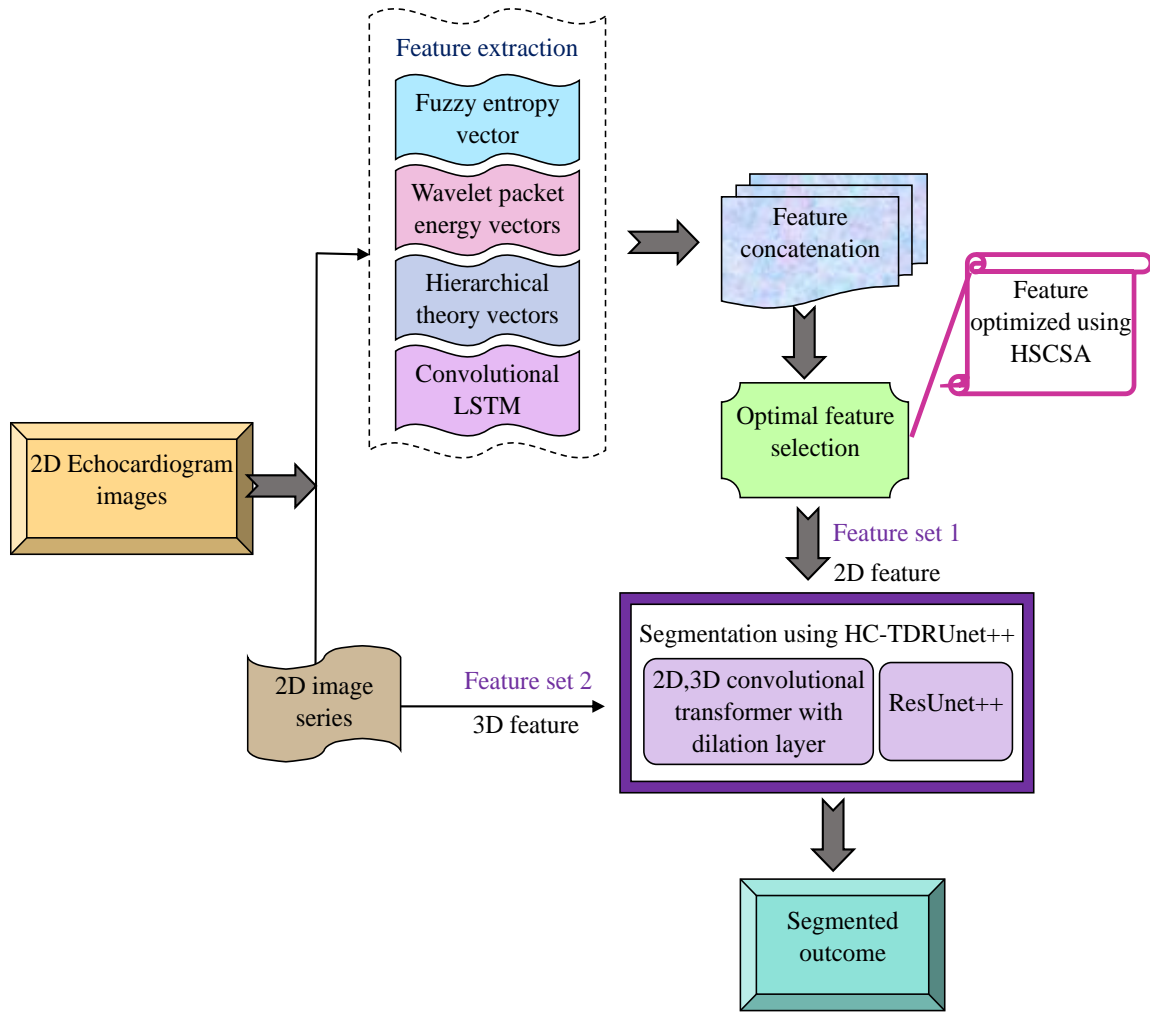


Fig. 2 Architectural diagram for the developed AF segmentation approach

This work suggested a deep learning based end-to-end framework for the automatic detection of Atrial Fibrillation. Initially, the required 2D Echocardiogram images are taken from the EchoNet-Dynamic database through the available link. The collected image has high-level semantic information, but utilizing individual feature extraction for several feature layers tends to affect the accuracy and result in information loss for small objects in the image. To leverage better feature information, this work uses different feature extraction

strategies and feature concatenation to generate the optimal feature selection. Fuzzy entropy vectors, wavelet packet energy vectors, hierarchical theory vectors, and deep features based on Conv-LSTM are the approaches that are successfully utilized for the feature selection process. A fuzzy entropy vector retains the specific characteristic from the given image series to enhance the detection performance under noisy conditions. The wavelet packet energy vector helps to extract the character feature at various resolutions. It only has a

minimum feature vector. Hierarchical feature vectors adopt the specific information from the given image and take out the spatial location information based on the feature map to enhance the ability of the information mining of the network. Conv-LSTM helps to manage the sequential feature with multiple temporal context information. From the different layers, the deep feature is inadequately extracted. Based on these techniques, effective feature extraction is done, and the significant features are identified. Further, these resultant features are concatenated, and optimal features are selected. Here, the concatenation is the procedure to combine the extracted features to get a single effective feature. From the concatenated feature, the optimal feature is selected using the proposed HSCSA algorithm. This process helps to remove all the redundant features from the concatenated feature to enhance the accuracy of the segmentation process. This process is executed by optimizing the concatenated feature using the HSCSA algorithm.

This algorithm is developed by combining the SSA and CSA optimization algorithms along with the adaptive mechanism. Further, the resultant optimal feature, which is in the form of 2D, is known to be feature set 1. Further, the original 2D echocardiogram, which contains several 2D image series combined to form the 3D feature and is known to be feature set 2, is given to the developed segmentation model. This work designed the HC-TDRUnet++ for effective segmentation. The model is constructed by involving two networks called the transformer and the RUnet++. The transformer network is designed with 2 convolution layers, such as 2D and 3D convolution, to process the input. Both feature sets 1 and 2 are given separately to the 2D and 3D convolution layers in the transformer network.

In addition, the dilation layer is further added to the convolution layer to enhance the size of the receptive field and minimize the spatial resolution. The transformer effectively did the image processing and subjected the resultant feature to the RUnet++ model. ResUnet++ integrates the merits of both the Unet++ framework and the residual connection to avoid the gradient disappearing and minimize the training time. In the end, the RUnet++ offered the segmented result. To evaluate the obtained segmented result, a comparative analysis is performed, and the outcome shows that the proposed framework achieves an accurate result.

## 4. Feature Extraction Process and Optimal Feature Selection with Hybrid Algorithm

### 4.1. Extraction of Divergent Features

Feature extraction is a significant process that effectively participates in image recognition. The extracted feature vector from the given images reflects the unique characteristic of the echocardiogram and results in better segmentation results. This work utilizes four different types of feature extraction, which are explained below.

Fuzzy entropy vector [25]: It is the approach used to minimize the dimension of the partial discharge feature. Shannon's definition is followed by the fuzzy entropy for the feature extraction. Let  $Af_s^{ec}$  be the collected 2D echocardiogram,  $s = 1, 2, 3, \dots, S$  which is redesigned by the embedded dimension using Equation (1) and generalized using Equation (2).

$$U_s^n = \{Af_s, Af_{s+1}, \dots, Af_{s+n-1}\} - af_0(s), s = 1, 2, \dots, M - n + 1 \quad (1)$$

$$Af_0(s) = n^{-1} \sum_{k=0}^{n-1} af(s+k) \quad (2)$$

Here  $U_s^n$  is the neighbor vector and the similar degree explained based on the fuzzy using Equation (3).

$$E_{sk} - \mu(e_{sk}^n, r) \quad (3)$$

The maximum absolute changes are specified as  $e_{sk}^n$ , and the term  $\mu(\cdot)$  is the fuzzy membership function. The fuzzy encoder of the image feature is determined using Equation (4).

$$FuEn(n, r) = \lim_{M \rightarrow \infty} [In\phi^n - In\phi^{n+1}(s)] \quad (4)$$

The fuzzy encoder vector is computed for all the image series, and the values are utilized as features  $Fu_s^{ec}$ .

Wavelet packet energy vectors [26]: The Wavelet packet energy-based feature extraction is to determine the wavelet from the set of basic wavelets according to a certain criterion. The process of searching for the wavelet packet energy is explained below.

Let  $Af_s^{ec}$  be the collected echocardiogram image, which has several image series. The measures are defined using Equation (5).

$$s(1, 2, \dots, S) = \sum_{j=1}^{M-1} \sum_{k=i+1}^M (s_j - s_k)^2 \quad (5)$$

Here, the parameter of the input image is evaluated by the energy ratio of the image wavelet based on the corresponding measures. The image dimension is indicated as  $y_j^m$ . The coefficient of the wavelet defined by the energy ratio based on the image is evaluated. The selection criterion of the wavelet packet is to increase the parameter measure. After the comparison is finished, the obtained decomposition coefficient evaluates the character feature, and it is termed as  $Wp_s^{ec}$ .

Hierarchical Theory Vectors [27]: This model takes the gathered image as input  $Af_s^{ec}$ . Further, it generates the different feature map scales based on  $s = 1, 2, 3, \dots, S$  and utilizes the corresponding operation for feature extraction. There are different scales and feature information contained in

the feature map block. This strategy separately evaluates the category information and the instance and incorporates them. Further, it discards the irrelevant feature, which minimizes the dimension of the extracted feature. The main purpose of this strategy is to fully mine the feature map information and improve the feature expression. It helps to develop the capability of recognition to easily evaluate the small-scale features. The hierarchical system minimizes the calculation time, also by ensuring the efficiency of the segmentation. The resultant feature obtained from the hierarchical theory vectors is indicated as  $Hi_s^{ec}$

**Conv-LSTM [28]:** This approach is generally implemented to evaluate the spatial-temporal information of the given images  $Af_s^{ec}$ . The conv-LSTM model is mainly designed to determine the spatial relationship of the given image. It is developed by combining the convolutional network with the LSTM for image feature extraction. Here, the spatial semantic feature is extracted using the convolutional framework, and the sequential structure is extracted using the LSTM model. The fully connected layer present in the LSTM is replaced with the convolutional layer to generate the sequential inference process. Let  $s = 1, 2, 3, \dots, S$  be the set of feature maps collected from the given image series. The operation of the Conv-LSTM is formulated using Equations (6), (7), and (8)

$$\begin{pmatrix} j_t \\ g_t \\ p_t \\ h_t \end{pmatrix} = \begin{pmatrix} \sigma \\ \sigma \\ \sigma \\ \tanh \end{pmatrix} \circ \begin{pmatrix} S_t \\ I_{t-1} \end{pmatrix} \quad (6)$$

$$D_t = j_t \theta h_t + g_t \theta D_{t-1} \quad (7)$$

$$I_t = p_t \theta \tanh(D_t) \quad (8)$$

The parameters in the Conv-LSTM and the sigmoid function are indicated as  $X$  and  $\sigma$ . The element-wise product is specified as  $\theta$ . The input gate is termed as  $j_t, g_t, p_t$  and  $h_t$ .

The cell state and the hidden state at every time step are indicated as  $D_t$  and  $H_t$ . Here, the input decides how much information flows into the cell state, and it is controlled by the forget gate. The effective information is propagated using the output gate  $Cl_s^{ec}$ .

#### 4.2. Novel HSCSA for Optimization

HSCSA is a hybrid optimization model, mainly designed for optimal feature selection with a powerful strategy.

**Purpose:** For the optimal feature selection, the corresponding resultant feature from the extraction process is optimized using the introduced HSCSA model. Here, the feature variable gets tuned to increase the relief score in the proposed system. In addition, it addresses the computational

complexities in the designed AF segmentation framework. With the help of optimal feature selection, improve the model performance and interpretability.

**Novelty:** HSCSA is designed by including the adaptive concept with the two standard algorithm models, SSA [29] and CSA [30]. The SSA is developed by the influence of the flying squirrels, especially the dynamic foraging character and the effective method of locomotion, such as gliding. It is the powerful nature-inspired optimization used for unconstrained numerical optimization issues. It prevents the process from being trapped in the local optimal solution. SSA is a type of directed search process; hence, the new solution is considered the best solution. With remarkable convergence, the SSA attained the global optimum solution. Similarly, the CSA is a kind of meta-heuristic approach developed by analyzing the characteristics of the flocks of crows. It is mainly designed to solve the scheduling issues.

It achieves better functionality in the time calculation and the optimal solution. It only has fewer parameters, which tends to be implemented more easily. It is more efficient for the search optimization issues. In addition, it can solve the discrete issue. Hence, these two optimizations are considered in the designed article. Although these models have multiple advantages, they also have some challenges.

Even though SSA offers effective performance, it tends to be complex for the multimodal function. Similarly, the CSA model is complex because of the requirement for huge memory and computational time. Hence, to solve the issue, the HSCSA is introduced by integrating the SSA and CSA algorithms. Here, multi-objective optimization problems are solved, and the convergence is maximized. The adaptive concept is initiated along with the algorithm integration to perform the optimization. The adaptive concept is derived using Equation (9).

$$Q = \frac{Cf}{(Wf + Mf) + (Cf + Bf)} \quad (9)$$

HSCSA is designed based on the different fitness functions. Here, the new random value is generated, and it is indicated as  $Q$ . Here, the current and best fitness function is specified by the term  $Cf$  and  $Bf$ . Similarly, the worst and mean fitness values are derived as  $Wf$  and  $Mf$ . Based on the above formulation, a new random value is generated for the HSCSA.

The challenges present in both the SSA and CSA are addressed by introducing the new random values, which are replaced in Equations (10) and (11). By using this formulation, if the value  $Q > 0.5$  is updated, update the SSA; else, update using CSA. The mathematical steps in the existing SSA and CSA to develop the HSCSA are defined as follows.



SSA [31]: It is a population-based algorithm, which is initiated with the random starting location of the flying squirrel. To fulfil their energy needs daily, the flying squirrels move forward to the acorn nut. The new location is generated by Equation (10).

$$Sq_n^{t+1} = \begin{cases} Sq_{nt}^t + e_g \times H_d \times (Sq_{at}^t - Sq_n^t) & Q \geq u_{dp} \\ randomlocation & Otherwise \end{cases} \quad (10)$$

Here, the term  $Sq_n^{t+1}$ , and  $H_d$  indicates the flying squirrel from the normal tree and the gliding constant value. The distance of random gliding is represented as  $e_g$ . The term  $Q$  represented the updated random value from Equation (9).

CSA [32]: It is an evolutionary process developed based on the natural behaviour of the crow. Each crow has a hiding location, and it remembers it. The position of the hidden place is computed using Equation (11).

$$y^{j,itr+1} = y^{j,itr} + Q \times g^{l,itr} \times (n^{i,itr} - y^{i,itr}) \quad (11)$$

Here, the long flight of the crow is indicated  $g^{l,itr}$  on the corresponding iteration. The replaced random value from Equation (9) is specified as  $Q$ . The term  $n^{i,itr}$  indicated the hiding place. The pseudocode of the implemented HSCSA is expressed in Algorithm 1.

**Algorithm 1: Developed HSCSA**

```

Input: Resultant concatenated feature
Output: Optimized features
Population initialization
Evaluate the fitness function
While the iteration starts
    New random value  $Q$  generation based on Equation (9)
    If  $Q > 0.5$ 
        Update using SSA
        Flying squirrel moved to the hickory tree from the acorn tree.
        Flying squirrels moved from the normal tree to the acorn tree.
        Flying squirrels moved from the normal tree to the hickory tree.
    else
        Update using CSA
        The new crow position is based on the hidden place.
        The new position in the search space for food storage
        New position updated
    end if
    Save the best solution
end while
Return the optimal solution
    
```

### 4.3. Concatenation and Optimal Feature Selection

It is beneficial to combine the extracted features and select the optimal feature to obtain a good performance in the segmentation.

**Feature Concatenation:** The feature extracted from the above procedure analyses the distinctive feature in the given raw image series and generates four features,  $Fu_s^{ec}$ ,  $Wp_s^{ec}$ ,  $Hi_s^{ec}$  and  $Cl_s^{ec}$ . To reduce the number of features and for better performance, feature concatenation is performed by preserving significant information. The concatenation is a function  $Cf_s^{ec} = \{Fu_s^{ec}, Wp_s^{ec}, Hi_s^{ec}, Cl_s^{ec}\}$ . The process of concatenating the extracted features makes the process more efficient and reduces the computational power. This process also helps to enhance the functionality of the further segmentation process and simplify the working procedure.

**Optimal Feature Selection:** It is the process of avoiding irrelevant features from the given concatenated feature. It improves the functionality by improving the relief score metrics. Even though the concatenated features are more effective, it might lead to the formation of redundant features as highly efficient features.

To avoid this, HSCSA is designed for optimal feature selection. HSCSA is employed to select the optimal feature that better characterizes the concatenated feature  $Cf_s^{ec}$ . It maximizes the relief score with the selected minimal number of features. This optimal selection of features helps to select the significant features that are necessary for the final segmentation process. Therefore, the process of feature optimization using the HSCSA is implemented. The objective function is derived using Equation (12)

$$OF = \underset{\{Cf_s^{ec}\}}{argmax} [ReSc] \quad (12)$$

Here, the optimized feature with the ranges of 1 to the number of features is represented as  $Cf_s^{ec}$ , and the relief score is specified as  $ReSc$ . The relief score helps to evaluate the feature score of each feature to select the better-scoring feature in the feature selection process. The relief score is derived using Equation (13).

$$ReSc = w_i - (y_i - s_i) + (y_i - d_i) \quad (13)$$

Here, the same and different class instance is indicated as  $s_i$  and  $d_i$ . The feature vector is indicated as  $y_i$ . The output from the optimal feature is indicated as  $Fs_s^{ec}$ , which is in the 1D form.

The resultant feature is obtained by determining the  $s \times f$ , in which the  $s$  is the collection of image series and  $f$  is the number of features. The obtained feature is in 2D form and is considered as feature set 1.



## 5. Segmentation Framework for Fibrosis Disease using Hybrid Convolution-Based Trans-Dilated Resunet++

### 5.1. ResUnet++ Model

ResUnet++ [32] is a combined neural network that integrates the strength of the residual network and the Unet++ for medical image segmentation. It coordinates the hierarchical feature extraction from the Unet++ with the residual unit in the residual network.

Here, the Unet++ is considered the basic structure that employs the skip pathway to join the encoder and decoder. A dense convolution block is used to map the decoder and encoder feature maps. Equation (14) defines the skip pathway determination.

$$y^{i,j} = \begin{cases} H\{y^{i-1/j}\}, & j = 0 \\ H\left\{\left[\int_{k=0}^{j-1} U(y^{i+1,j-1})\right]\right\} & j > 0 \end{cases} \quad (14)$$

Here, the convolution operation is indicated as  $H\{\cdot\}$ . The node  $Y^{i,j}$  output is represented as  $y^{i,j}$ . The dense block convolution layer and the down-sampling layer are specified as  $j$  and  $i$ . Further, the up-sampling operation is indicated as  $u(\cdot)$ . The skip pathway is the residual structure connection that transfers the feature map from one layer to another deep layer. The encoder and decoder feature map is enhanced by the Unet++ model, and the network training is improved by the residual block to solve the degradation challenges. The overall framework of the ResUnet++ model is shown in Figure 3.

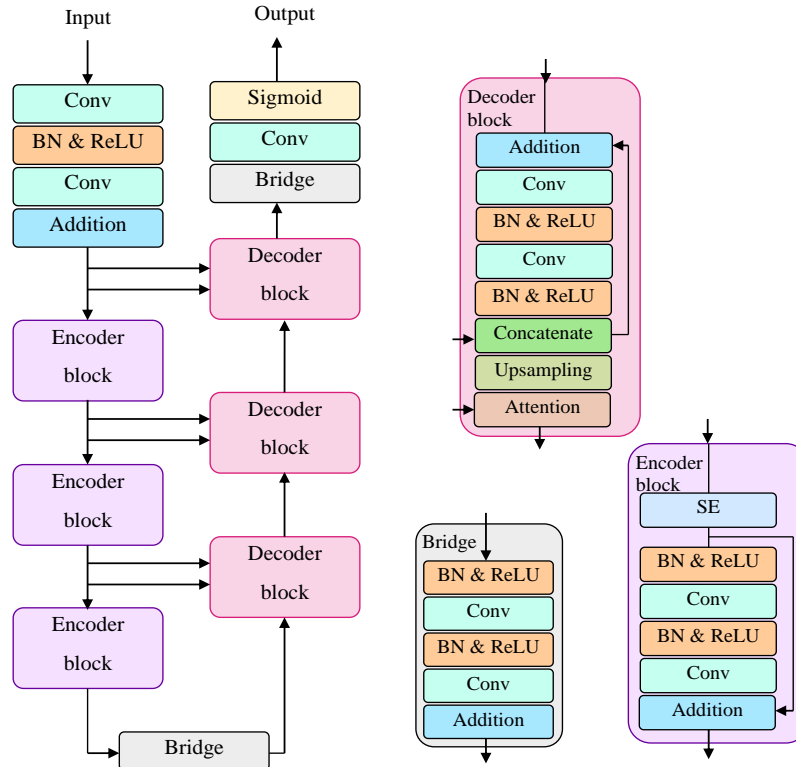


Fig. 3 Structural diagram of ResUnet++

### 5.2. Developed HC-TDRUnet++ for Segmentation

For achieving effective segmentation for determining Atrial Fibrosis, HC-TDRUnet++ is implemented in this work. This technique is designed by the integration of the Transformer network along with the ResUnet++, in which it performs the segmentation. Transformer Network [33]: It consists of an encoder and decoder with the implementation of the attention mechanism. The network has eight identical layers that stack on top of each other. For every identical layer, there is a sub-layer, which is a multi-head attention layer and a fully connected layer. The residual network is used to connect those layers. For the attention function, the inputs are

value, key, and query, and are indicated as  $U$ ,  $J$  and  $P$ . The query key similarity is used to calculate the attention weight and is measured using Equation (15).

$$At(P, J, U) = Sfm(PJ_T / \sqrt{c_j}U) \quad (15)$$

Here, the attention mechanism and the softmax are specified as  $At$  and  $Sfm$ . Different linear transformations are used by the multi-head attention to project the  $U$ ,  $J$  and  $P$  to achieve the attention outcome, and it is formulated using Equation (16).

$$Mh(P, J, U) = Cc(hd_1, \dots, hd_g) \quad (16)$$

Here, the multi-head, concatenation, and the number of heads are represented as  $Mh, C$  and  $hd$ , where each head is determined using Equation (17).

$$hd_h = At(PV_h^P, JV_h^J, UV_h^U) \quad (17)$$

In the encoder, each layer is provided with a fully connected feed-forward network, and the linear transformation is managed based on the ReLU using Equation (18).

$$FFN(w) = \max(0, wV_1 + a_1)V_2 + a_2 \quad (18)$$

In addition, the position encoding is used to order the sequence, which tends to embed the input at the top of the encoder.

Dilation [34]: It is involved mainly in addressing challenges like information loss and resolution reduction in image processing. In general, the convolution layer present in the network improves the local receptive field, which tends to narrow the feature map size.

The process of minimizing the size of the feature map causes a reduction in accuracy and tends to lose significant information. To address this issue, a dilation mechanism is developed, which maintains a similar number of parameters even for the large receptive field.

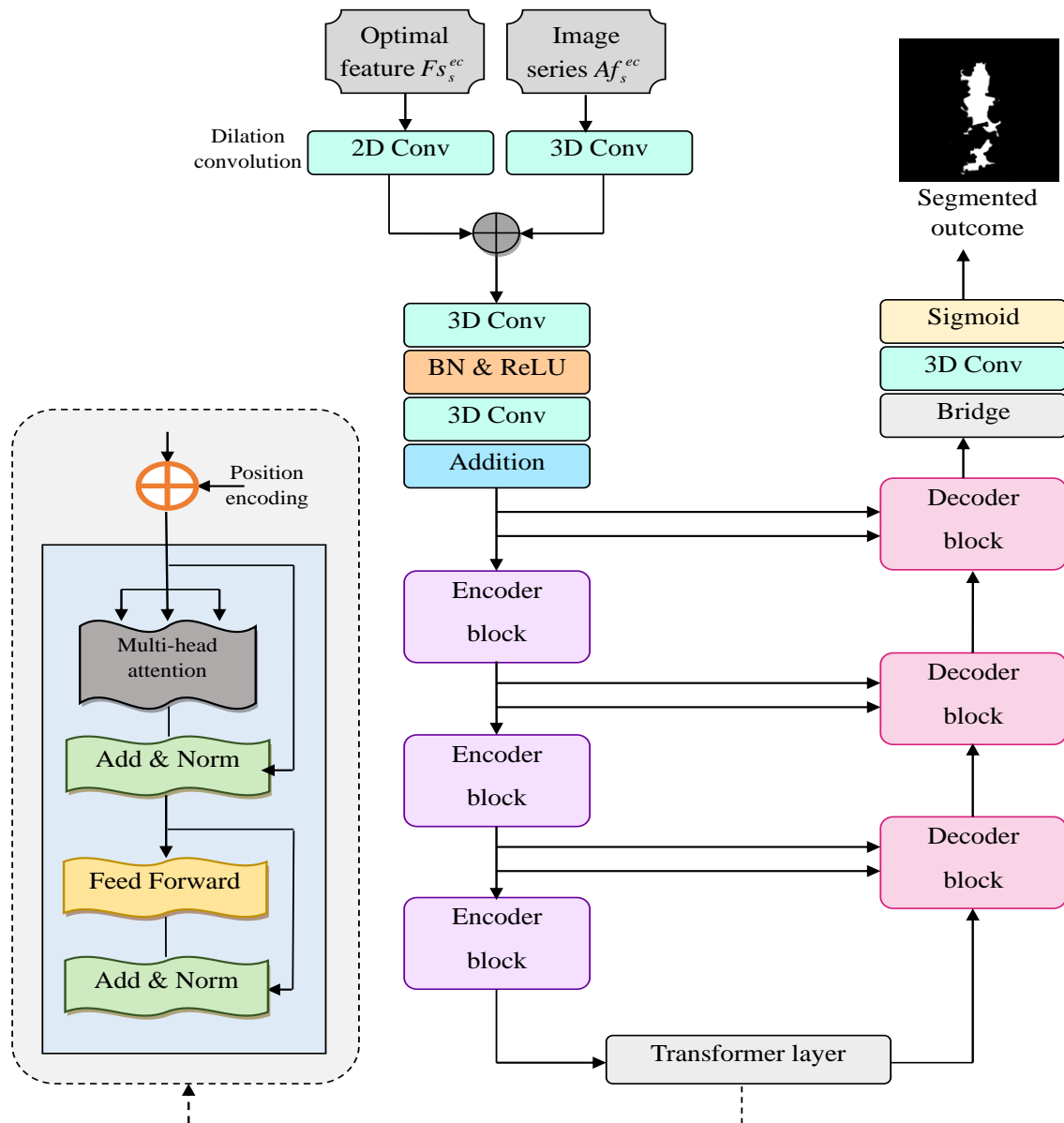


**Fig. 4 Illustration for proposed HC-TDRUnet++ for segmentation**

HC-TDRUnet++: This model is developed by two combinational networks, in which RUnet++ is considered the basic network. Here, the transformer network is used, which contains the 2D and 3D convolution along with the dilation layer to discriminate the effective feature.

The resultant optimal feature  $Fs_s^{ec}$  (feature set 1) and the extracted image series  $Af_s^{ec}$  (feature set 2) are given as input to the HC-TDRUnet++ model. The input is in the form of a 2D and 3D structure.

Similarly, the transformer layer in the network is constructed by involving the 2D and 3D convolution along with the dilation layer for image processing. Initially, the input is subjected to the transformer layer, where the optimal feature is given to the 2D convolution. Similarly, the collected 2D image series, combined to form the 3D feature, are given to the 3D convolution. The given feature was convolved in the 2D convolution and resulted in the extraction of the feature map. Similarly, the 3D convolution takes out the spatial and temporal patterns in the given image series.

Here, the first axis is used to determine the time direction, whereas the second and third axes are used for the spatial dimension of the image series. In addition, the dilation mechanism is added to the convolution, which helps in incorporating the diverse receptive fields.

This mechanism enhances the extraction process by enabling multi-scale information. The multi-head attention part involved in the network improves the network's capability and analyzes the diverse relations among the input.

The extracted feature from the transformer network is given to the final segmentation model called RUnet++. The introduced segmentation model is the combination of the residual network and the Unet++ model. Here, the residual connection is added to the general Unet++ model, in which the residual unit solves the degradation problem.

The Unet++ enhances the semantic gap between the encoder and decoder feature maps. In the end, the RUnet++ segments the desired target accurately. The structural representation of the proposed HC-TDRUnet++ for segmentation is shown in Figure 4.

## 6. Results and Discussion

### 6.1. Experimental Setup

The developed atrial fibrosis segmentation approach using deep learning was implemented in Python, and the analysis was carried out. The initialization of HSCSA was designed by using the population number of 10, a chromosome length, and a maximum iteration of 50. Other classical algorithms like "Addax Optimization Algorithm (AOA) [35], Rock Hyraxes Swarm Optimization (RHSA) [36], SSA [30], and CSA [31]" were employed. Similarly, other classifiers, such as UNet [21], Multilabel CNN [22], ResNet [23], and DBN [24], were also considered.

### 6.2. Evaluation Metrics

Accuracy, dice coefficient, and the Jaccard were determined using Equations (19), (20), and (21).

$$Ac = \frac{X^p + X^n}{X^p + X^n + Y^p + Y^n} \quad (19)$$

$$Dic = \frac{2X^p}{2X^p + Y^p + Y^n} \quad (20)$$

$$Jacc = \frac{X^p}{X^p + Y^n + Y^p} \quad (21)$$

Mean Squared Error (MSE) and the Peak Signal to Noise Ratio PSNR are formulated using Equation (22) and (23).

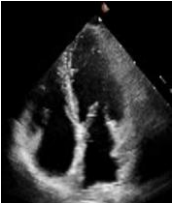
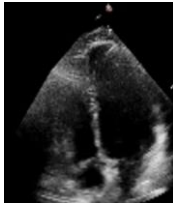
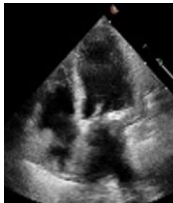
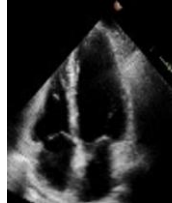
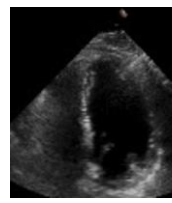
$$MSE = \sum (a_i - h_i)^2 m \quad (22)$$

$$PSNR = 10 \times \log_{10} \frac{Q^2}{\frac{1}{N} \sum (z(i) - \hat{z}(i))^2} \quad (23)$$

Here, the true positive and the false positive are specified as  $X^p$  and  $Y^p$ . True negative and false negative are represented as  $X^n$  and  $Y^n$ . The number of observations is indicated as  $m$ , the observed and predicted value represented as  $a_i$  and  $h_i$ . The term  $Q$  is the maximum pixel value, and the term  $N$  is the number of pixels.

### 6.3. Image Result of the Designed HC-TDRUnet++ for Atrial Fibrosis Segmentation

The collected image series from the presented dataset is segmented using the suggested HC-TDRUnet++ model. The resultant image from the HC-TDRUnet++ is compared with the other segmentation model defined in Figure 5.

Description	1	2	3	4	5
Dataset 1					
Original image					

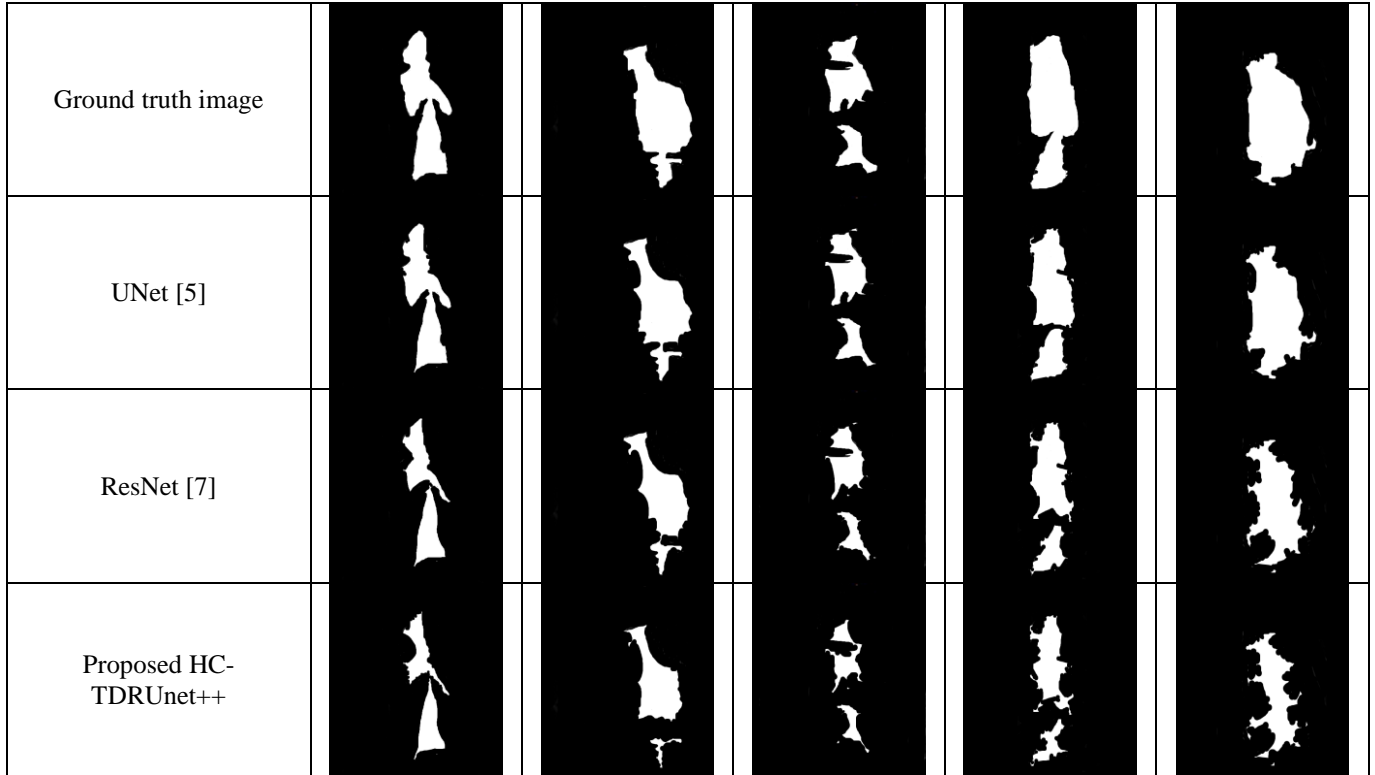


Fig. 5 Resultant segmentation image based on the esigned HC-TDRUnet++

#### 6.4. Convergence Analysis of the Designed HSCSA Optimization

The convergence analysis of the initiated HSCSA optimization contrasted with the earlier heuristic algorithm defined in Figure 6. Here, the number of iterations is varied to analyze the convergence assessment for the presented algorithm. Based on this analysis, the cost function value varied. The better convergence is achieved by lowering the cost function value. This analysis helps to evaluate the better convergence of the optimization model.

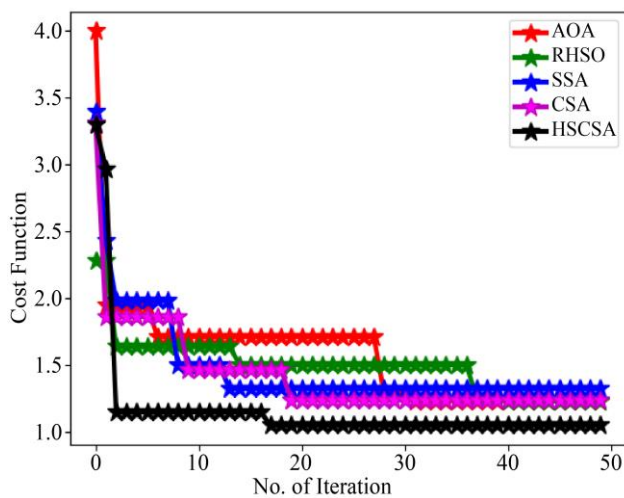


Fig. 6 Convergence analysis of the suggested HSCSA over existing algorithms

It helps to solve the optimization challenges and offer the optimal solution. By taking the number of iterations as 20, the developed HSCSA model attained the maximum convergence of 80% of AOA, 50% of RHSO, 30% of SSA, and 20% of CSA.

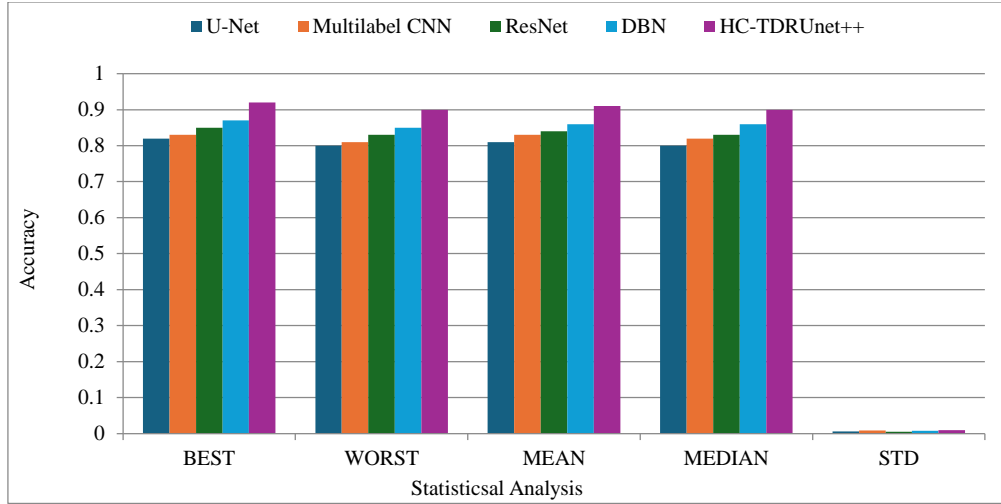
From the graphical result, the HSCSA achieved higher convergence, which tends to offer the optimal solution.

#### 6.5. Performance Analysis of the Proposed HC-TDRUnet++ based Segmentation

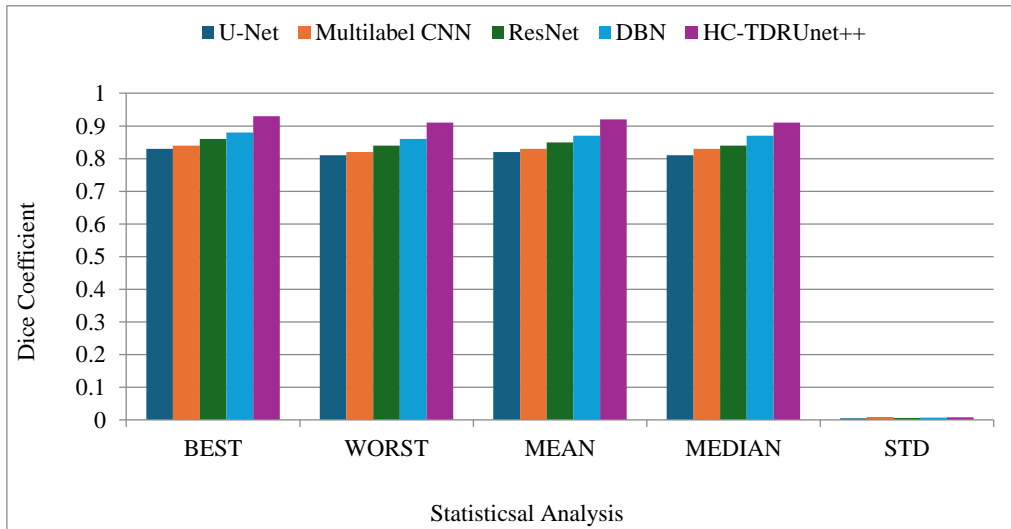
The performance determination of the proposed HC-TDRUnet++ based segmentation model compared with the available classifiers is defined in Figure 7. Here, different statistical measures are used to evaluate the functionality of the classifier.

Various measures like the accuracy, PSNR, Jaccard, dice coefficient, and MSE are used to evaluate the function. The statistical measures varied as best, worst, median, mean, and standard deviation.

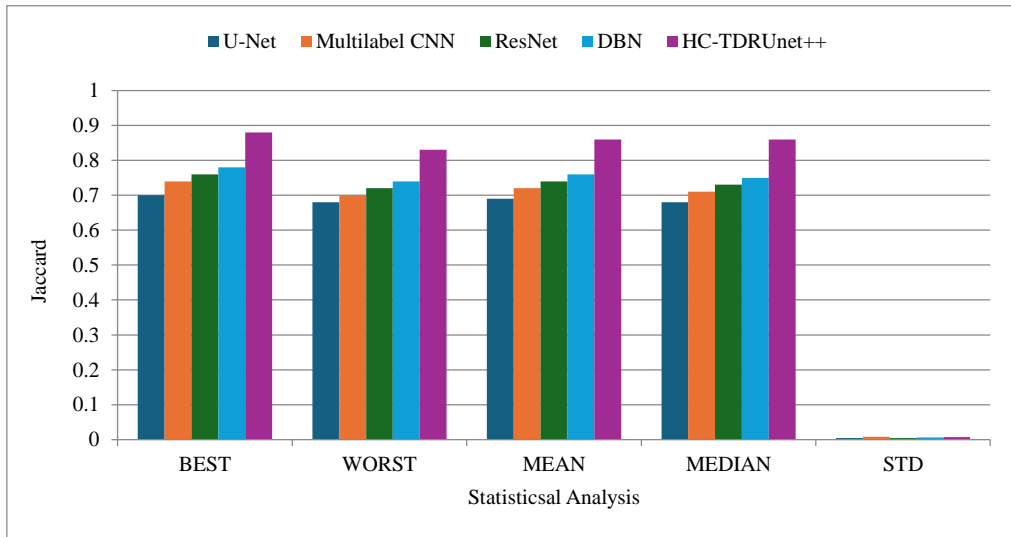
From the analysis, the accuracy of the HC-TDRUnet++ model was enhanced to 7.7% of UNet, 6.6% of Multilabel CNN, 5.5% of ResNet, and 4.4% of DBN by taking the best measures. From the result, it is noted that the proposed approach attained higher accuracy in the segmentation process than the other classifiers



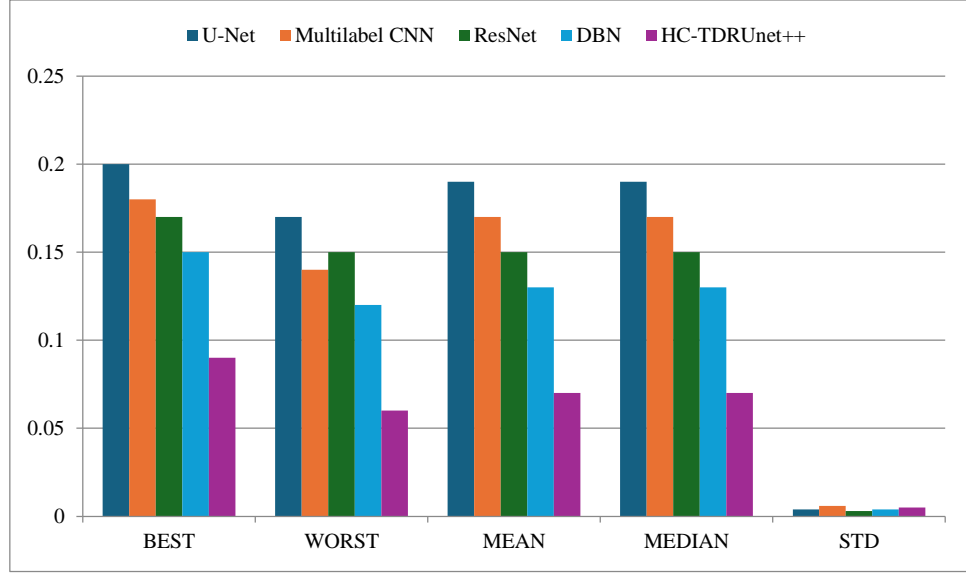
(a)



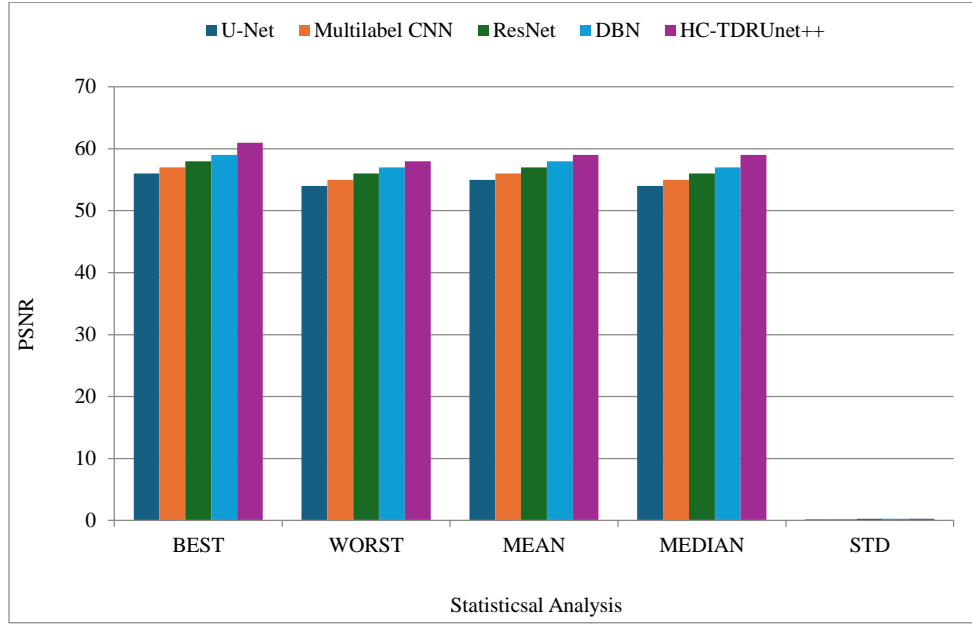
(b)



(c)



(d)



(e)

**Fig. 7 Performance analysis of the implemented HC-TDRUnet++ based segmentation differentiated with other existing classifiers regarding (a) Accuracy, (b) Dice coefficient, (c) Jaccard, (d) MSE, and (e) PSNR.**

#### 6.5.1. Epoch-Based Performance Evaluation of the Designed HC-TDRUnet++-Based Segmentation

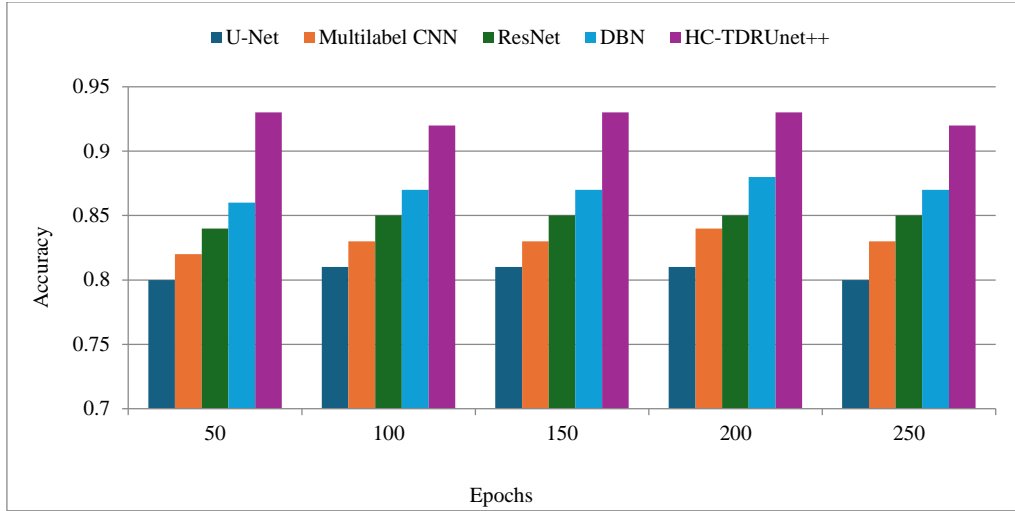
The functionality assessment of the designed segmentation model is determined using the epoch value analysis defined in Figure 8.

Here, various metrics are used under the given dataset to perform the comparative analysis.

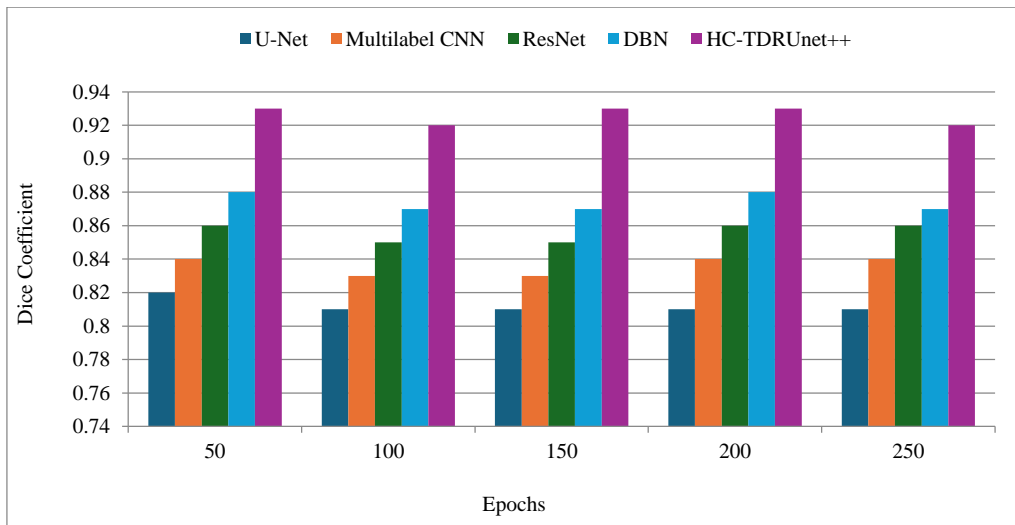
The epoch value is varied to validate the performance of the model.

The epoch value ranges from 50 to 250 to evaluate the performance of the segmentation approach. Based on the graphical analysis, the suggested model achieved a greater result than 15.7% of UNet, 12.6% of Multilabel CNN, 10.5% of ResNet, and 8.4% of DBN by taking the epoch value as 50.

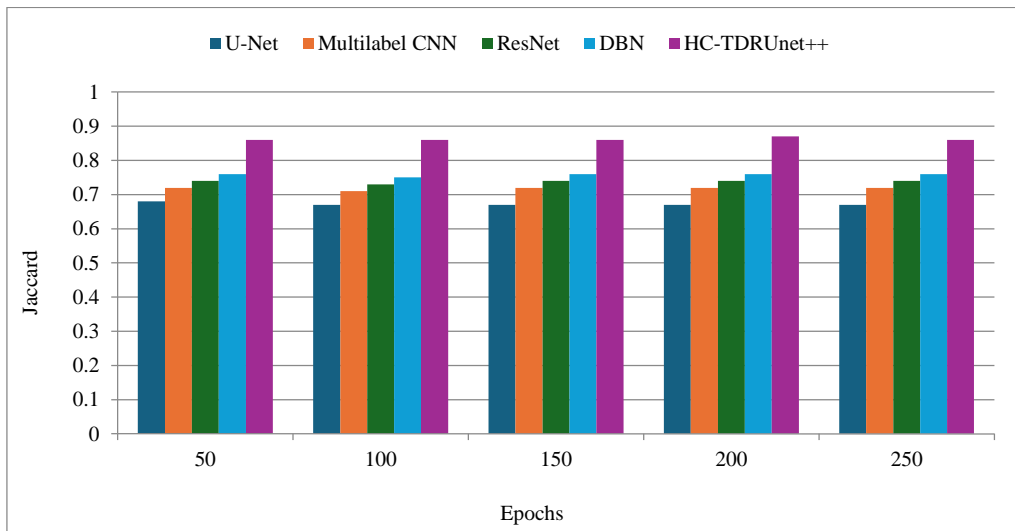
From the calculation, the superior functionality is achieved by the designed approach for medical image segmentation. From the result, the designed model has a better outcome than the existing techniques.



(a)

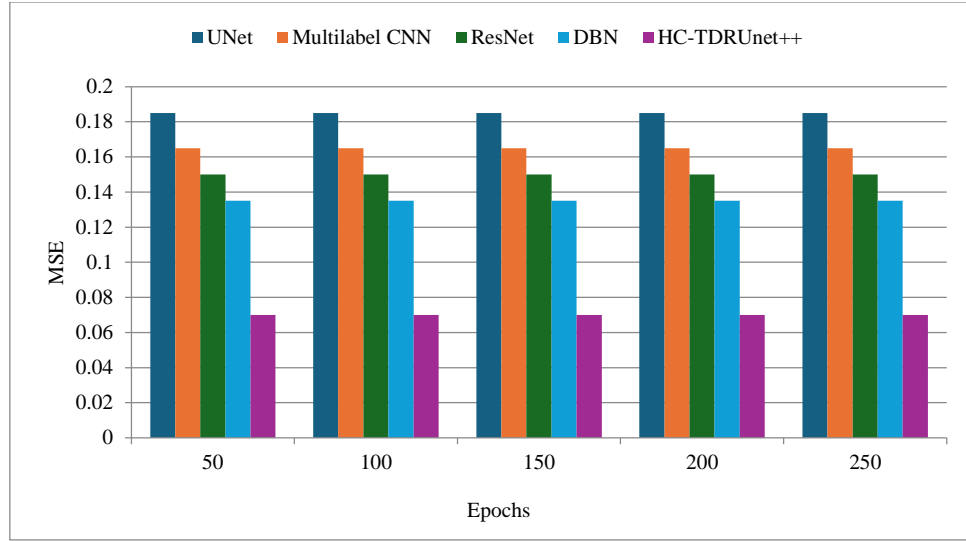


(b)

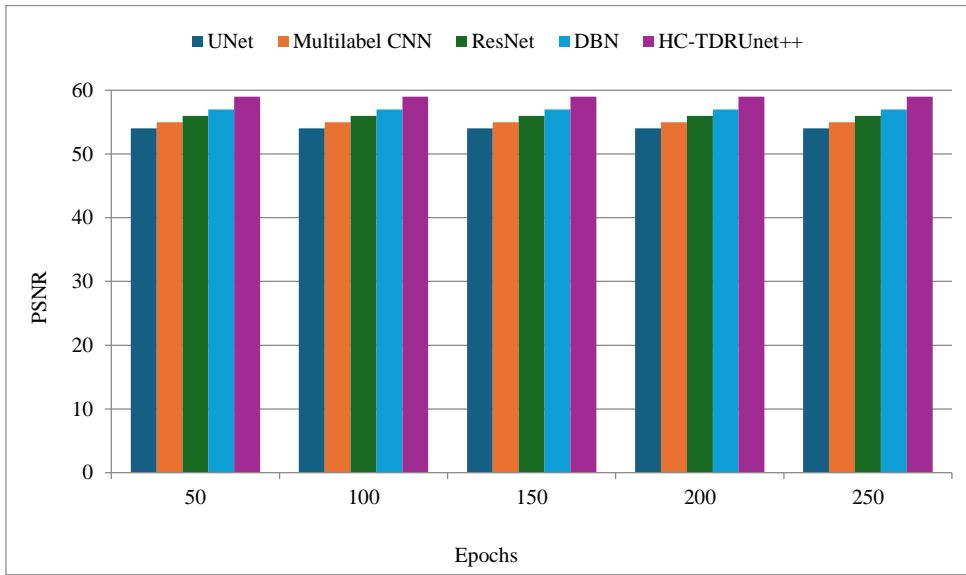


(c)





(d)



(e)

Fig. 8 Epoch-based performance analysis of the suggested HC-TDRUnet++ based segmentation compared with the earlier model by determining the mean value regarding (a) Accuracy, (b) Dice coefficient, (c) Jaccard, (d) MSE, and (e) PSNR.

#### 6.6. Statistical Analysis of the Introduced Hybrid Algorithm

The efficiency of the presented HSCSA optimization model compared with the previous algorithm is based on the statistical evaluation expressed in Table 2. From the table result, it is obtained that the constant improvement achieved by the HSCSA optimization is different from that of the other

algorithms. The functionality of the algorithm is enhanced to offer the optimal solution. From the table result, the proposed HSCSA achieved a higher value than 17.4% of AOA, 17.4% of RHO, 26.3% of SSA, and 18.1% of CSA by taking the best measures. By comparing the existing optimization model, the implemented HSCSA achieved an effective result.

Table 2. Statistical analysis of the proposed HSCSA compared with the traditional algorithm

Terms	AOA [35]	RHO [36]	SSA [30]	CSA [27]	HSCSA
“Best”	1.228707	1.228739	1.32221	1.236647	1.046597
“Worst”	3.99594	2.274783	3.393012	3.305861	3.294731
“Mean”	1.571094	1.492875	1.482287	1.422783	1.159962
“Median”	1.710059	1.498442	1.32221	1.236647	1.046597
“Standard deviation”	0.435169	0.216626	0.373485	0.350929	0.406268

### 6.7. Overall Analysis of the Designed Segmentation Model

By determining the best and standard deviation measures, the overall validation of the proposed HC-TDRUnet++ model is obtained. Here is the overall comparison of the proposed segmentation technique with the existing classifier, as shown in Table 3.

Based on the best measure, the implemented HC-TDRUnet++ value is enhanced over 11.9% of UNet, 9.6% of Multilabel CNN, 8.5% of ResNet, and 6.8% of DBN by taking the accuracy measure. From the result, it is noted that the proposed segmentation approach attains more effective and accurate segmentation than other techniques.

**Table 3. Overall analysis of the recommended atrial fibrosis segmentation model compared with the existing classifier**

Terms	UNet [21]	CNN [22]	ResNet [23]	DBN [24]	HC-TDRUnet++
<b>Dice Coefficient</b>	8.290422	8.556669	8.634486	8.781093	9.400049
<b>Jaccard</b>	7.080034	7.477429	7.597092	7.827049	8.868012
<b>Accuracy</b>	8.283691	8.495026	8.598022	8.76297	9.404449
<b>PSNR</b>	55.78485	56.35551	56.66339	57.207	60.38162
<b>MSE</b>	1.984863	1.822052	1.628113	1.512604	0.887756

## 7. Conclusion

AF generates severe health consequences, which can lead to death. Therefore, an effective method for segmenting Atrial Fibrosis could have an advantageous medical impact by allowing the detection of AF in patients. This work initiated the deep learning architecture to perform the segmentation of Atrial Fibrosis based on the echocardiogram image series, which were in 2D form. The feature extraction process was conducted to take out the effective feature by using fuzzy entropy, wavelet packet energy, hierarchical theory, and convolutional LSTM. The resultant features from each process were concatenated, and further, the optimal feature was based on the HSCSA.

The 2D optimal feature and the 3D feature were subjected to the HC-TDRUnet++ for the segmentation process. The developed model has effective segmentation and achieved an accurate result.

The accuracy of the HC-TDRUnet++ model was enhanced by 19.6% of UNet, 12% of Multilabel CNN, 36.8% of ResNet, and 0.7% of DBN, respectively. From the result, the suggested approach performed successful segmentation, and it was capable of performing the quick AF segmentation. In the future, the recommended model will be extended to better classify the AF in the early stage to avoid stroke and decrease the death rate.

## References

- [1] Nabil Naser, Ivan Stankovic, and Aleksandar Neskovic, "The Reliability of Automated Three-Dimensional Echocardiography-HeartModel<sup>A1</sup> Versus 2D Echocardiography Simpson Methods in Evaluation of Left Ventricle Volumes and Ejection Fraction in Patients with Left Ventricular Dysfunction," *Medical Archives*, vol. 76, no. 4, pp. 259-266, 2022. [[CrossRef](#)] [[Google Scholar](#)] [[Publisher Link](#)]
- [2] Decai Zeng et al., "Machine Learning Model for Predicting Left Atrial Thrombus or Spontaneous Echo Contrast in Non-Valvular Atrial Fibrillation Patients based on Multimodal Echocardiographic Parameters," *medRxiv*, pp. 1-32, 2024. [[CrossRef](#)] [[Google Scholar](#)] [[Publisher Link](#)]
- [3] N. Lu et al., "New Deep Learning Approach for Automated Diagnosis of Atrial Fibrillation by Echocardiography Without Ecg," *Canadian Journal of Diabetes*, vol. 39, no. 10, pp. s217-s218, 2023. [[CrossRef](#)] [[Google Scholar](#)] [[Publisher Link](#)]
- [4] Saroj Kumar Pandey et al., "Automatic Detection of Atrial Fibrillation from ECG Signal using Hybrid Deep Learning Techniques," *Journal of Sensors*, vol. 2022, pp. 1-11, 2022. [[CrossRef](#)] [[Google Scholar](#)] [[Publisher Link](#)]
- [5] E.K. Mounika et al., "Quantum Feature Pruning for Scalable and Efficient Quantum Kernel-Based High-Dimensional Classification," *2025 International Conference on Inventive Computation Technologies (ICICT)*, Kirtipur, Nepal, pp. 1412-1420, 2025. [[CrossRef](#)] [[Google Scholar](#)] [[Publisher Link](#)]
- [6] Solomon Osarumwense Alile, "An Ischemic Heart Disease Prediction Model based on Observed Symptoms using Machine Learning," *International Journal of Computer Engineering in Research Trends*, vol. 7, no. 9, pp. 9-23, 2020. [[Google Scholar](#)] [[Publisher Link](#)]
- [7] Sarah W.E. Baalman et al., "A Morphology based Deep Learning Model for Atrial Fibrillation Detection using Single Cycle Electrocardiographic Samples," *International Journal of Cardiology*, vol. 316, pp. 130-136, 2020. [[CrossRef](#)] [[Google Scholar](#)] [[Publisher Link](#)]
- [8] P. SumanPrakash et al., "Learning-Driven Continuous Diagnostics and Mitigation Program for Secure Edge Management Through Zero-Trust Architecture," *Computer Communications*, vol. 220, pp. 94-107, 2024. [[CrossRef](#)] [[Google Scholar](#)] [[Publisher Link](#)]
- [9] Yunfan Chen et al., "Atrial Fibrillation Detection using a Feedforward Neural Network," *Journal of Medical and Biological Engineering*, vol. 42, no. 1, pp. 63-73, 2022. [[CrossRef](#)] [[Google Scholar](#)] [[Publisher Link](#)]
- [10] Amin Ullah et al., "Classification of Arrhythmia by using Deep Learning with 2-D ECG Spectral Image Representation," *Remote Sensing*, vol. 12, no. 10, pp. 1-14, 2020. [[CrossRef](#)] [[Google Scholar](#)] [[Publisher Link](#)]

- [11] Li Jiahao et al., "An End-End Arrhythmia Diagnosis Model based on Deep Learning Neural Network with Multi-Scale Feature Extraction," *Physical and Engineering Sciences in Medicine*, vol. 46, no. 3, pp. 1341-1352, 2023. [[CrossRef](#)] [[Google Scholar](#)] [[Publisher Link](#)]
- [12] Yonggang Zou et al., "A Generalizable and Robust Deep Learning Method for Atrial Fibrillation Detection from Long-Term Electrocardiogram," *Biomedical Signal Processing and Control*, vol. 90, 2024. [[CrossRef](#)] [[Google Scholar](#)] [[Publisher Link](#)]
- [13] R. Anand et al., "An Enhanced Resnet-50 Deep Learning Model for Arrhythmia Detection using Electrocardiogram Biomedical Indicators," *Evolving Systems*, vol. 15, no. 1, pp. 83-97, 2024. [[CrossRef](#)] [[Google Scholar](#)] [[Publisher Link](#)]
- [14] Yong-Soo Baek et al., "A New Deep Learning Algorithm of 12-Lead Electrocardiogram for Identifying Atrial Fibrillation During Sinus Rhythm," *Scientific Reports*, vol. 11, no. 1, pp. 1-10, 2021. [[CrossRef](#)] [[Google Scholar](#)] [[Publisher Link](#)]
- [15] Jianxin Xie, Stavros Stavrakis, and Bing Yao, "Automated Identification of Atrial Fibrillation from Single-Lead ECGs using Multi-Branching Resnet," *Frontiers in Physiology*, vol. 15, pp. 1-17, 2024. [[CrossRef](#)] [[Google Scholar](#)] [[Publisher Link](#)]
- [16] Xiangyu Zhao et al., "Atrial Fibrillation Detection with Single-Lead Electrocardiogram based on Temporal Convolutional Network-ResNet," *Sensors*, vol. 24, no. 2, pp. 1-14, 2024. [[CrossRef](#)] [[Google Scholar](#)] [[Publisher Link](#)]
- [17] Neal Yuan et al., "Deep Learning Evaluation of Echocardiograms to Identify Occult Atrial Fibrillation," *npj Digital Medicine*, vol. 7, no. 1, pp. 1-8, 2024. [[CrossRef](#)] [[Google Scholar](#)] [[Publisher Link](#)]
- [18] Bambang Tutuko et al., "Afibnet: An Implementation of Atrial Fibrillation Detection with Convolutional Neural Network," *BMC Medical Informatics and Decision Making*, vol. 21, no. 1, pp. 1-17, 2021. [[CrossRef](#)] [[Google Scholar](#)] [[Publisher Link](#)]
- [19] Luigi Di Biase et al., "Feasibility of Three-Dimensional Artificial Intelligence Algorithm Integration with Intracardiac Echocardiography for Left Atrial Imaging During Atrial Fibrillation Catheter Ablation," *EP Europace*, vol. 25, no. 9, pp. 1-7, 2023. [[CrossRef](#)] [[Google Scholar](#)] [[Publisher Link](#)]
- [20] Luan Tran et al., "Multifusionnet: Atrial Fibrillation Detection with Deep Neural Networks," *AMIA Summits on Translational Science Proceedings*, pp. 654-663, 2020. [[Google Scholar](#)] [[Publisher Link](#)]
- [21] Xin Liu et al., "Deep Learning-Based Automated Left Ventricular Ejection Fraction Assessment using 2-D Echocardiography," *American Journal of Physiology-Heart and Circulatory Physiology*, vol. 321, no. 2, pp. H390-H399, 2021. [[CrossRef](#)] [[Google Scholar](#)] [[Publisher Link](#)]
- [22] Orod Razeghi et al., "Fully Automatic Atrial Fibrosis Assessment using a Multilabel Convolutional Neural Network," *Circulation: Cardiovascular Imaging*, vol. 13, no. 12, pp. 1-11, 2020. [[CrossRef](#)] [[Google Scholar](#)] [[Publisher Link](#)]
- [23] Nelson Lu et al., "Automated Atrial Fibrillation Diagnosis by Echocardiography without ECG: Accuracy and Applications of a New Deep Learning Approach," *Diseases*, vol. 12, no. 2, pp. 1-10, 2024. [[CrossRef](#)] [[Google Scholar](#)] [[Publisher Link](#)]
- [24] Alugonda Rajani, and Sai Lakshmi Dangeti, "Accuracy Enhancement during Atrial Fibrillation Detection using Hybrid Machine Learning Algorithm and Echo Peak Detection Algorithm," *International Conference on Recent Advances in Deep Learning (ICRADL-2021)*, Kakinada, India, vol. 9, no. 5, pp. 389-393, 2021. [[Google Scholar](#)] [[Publisher Link](#)]
- [25] S. Mounika et al., "Heart Disease Prediction using Machine Learning with Recursive Feature Elimination for Optimized Performance," *International Journal of Computer Engineering in Research Trends*, vol. 11, no. 1s, pp. 61-67, 2024. [[Publisher Link](#)]
- [26] Wei Huang, Xiaobo Lu, and Xiaojing Ling, "Wavelet Packet based Feature Extraction and Recognition of License Plate Characters," *Chinese Science Bulletin*, vol. 50, no. 2, pp. 97-100, 2005. [[CrossRef](#)] [[Google Scholar](#)] [[Publisher Link](#)]
- [27] Di Wang et al., "Hfenet: Hierarchical Feature Extraction Network for Accurate Landcover Classification," *Remote Sensing*, vol. 14, no. 17, pp. 1-24, 2022. [[CrossRef](#)] [[Google Scholar](#)] [[Publisher Link](#)]
- [28] Linwei Ye, Zhi Liu, and Yang Wang, "Dual Convolutional LSTM Network for Referring Image Segmentation," *IEEE Transactions on Multimedia*, vol. 22, no. 12, pp. 3224-3235, 2020. [[CrossRef](#)] [[Google Scholar](#)] [[Publisher Link](#)]
- [29] Zijian Zhao et al., "Kolmogorov-Arnold-Based Network with Lightweight Feature Fusion Schema for Single-Lead Electrocardiogram Atrial Fibrillation Detection," *2024 IEEE 24<sup>th</sup> International Conference on Bioinformatics and Bioengineering (BIBE)*, Kragujevac, Serbia, pp. 1-6, 2024. [[CrossRef](#)] [[Google Scholar](#)] [[Publisher Link](#)]
- [30] Mohit Jain, Vijander Singh, and Asha Rani, "A Novel Nature-Inspired Algorithm for Optimization: Squirrel Search Algorithm," *Swarm and Evolutionary Computation*, vol. 44, pp. 148-175, 2019. [[CrossRef](#)] [[Google Scholar](#)] [[Publisher Link](#)]
- [31] Antono Adhi, Budi Santosa, and Nurhadi Siswanto, "A Meta-Heuristic Method for Solving Scheduling Problem: Crow Search Algorithm," *IOP Conference Series: Materials Science and Engineering, International Conference on Industrial and Systems Engineering (IconISE)*, Denpasar, Bali, Indonesia, vol. 337, pp. 1-6, 2018. [[CrossRef](#)] [[Google Scholar](#)] [[Publisher Link](#)]
- [32] R. Johny Elton et al., "Voice Activity Detection using Smoothed-Fuzzy Entropy (Smfuzzyen) and Support Vector Machine," *Journal of Applied Research and Technology*, vol. 17, no. 1, pp. 8-19, 2019. [[CrossRef](#)] [[Google Scholar](#)] [[Publisher Link](#)]
- [33] Chao Che et al., "Constrained Transformer Network for ECG Signal Processing and Arrhythmia Classification," *BMC Medical Informatics and Decision Making*, vol. 21, no. 1, pp. 1-13, 2021. [[CrossRef](#)] [[Google Scholar](#)] [[Publisher Link](#)]
- [34] Lirong Yin et al., "Convolution-Transformer for Image Feature Extraction," *CMES-Computer Modeling in Engineering and Sciences*, vol. 141, no. 1, pp. 87-106, 2024. [[CrossRef](#)] [[Google Scholar](#)] [[Publisher Link](#)]

- [35] Tareq Hamadneh et al., “Addax Optimization Algorithm: A Novel Nature-Inspired Optimizer for Solving Engineering Applications,” *International Journal of Intelligent Engineering and Systems*, vol. 17, no. 3, pp. 732-743, 2024. [[CrossRef](#)] [[Google Scholar](#)] [[Publisher Link](#)]
- [36] Belal Al-Khateeb et al., “Rock Hyraxes Swarm Optimization: A New Nature-Inspired Metaheuristic Optimization Algorithm,” *Computers, Materials and Continua*, vol. 68, no. 1, pp. 643-654, 2021. [[CrossRef](#)] [[Google Scholar](#)] [[Publisher Link](#)]